JOURNAL OF MATERIALS SCIENCE **30** (1995) 4598–4602

Low-temperature fracture toughness study of Fe–7Al–27Mn–C alloys

YIN-BEAN CHANG, SHEN-CHIH LEE*, CHIA-JUNG HU*
*Departments of Mechanical Engineering and *Materials Engineering, Tatung Institute Technology, Taipei, Taiwan*

This research studied the fracture toughness of the Fe–7Al–27Mn alloys with increasing carbon contents: 0.5% C, Fl alloy: 0.7% C, F2 alloy (with 4.0% Cr); and 1.0% C, F3 alloy. Fracture toughness experiments were conducted at temperatures of 25, − 50, − 100 and − 150 °C. It was found that plane-stress, K_C, values as measured by the R-curve method, decreased as the temperature dropped. F1 alloy possessed the highest K_C value at all temperatures among the three alloys. The K_C values of the F2 and F3 alloys were similar at ambient temperatures, but F3 maintained the toughness property and ductility better at sub-zero temperatures. Quantitatively, K_C values of the F2 alloy at − 150 °C were ca. 60% less than at 25 °C, but F1 and F3 alloys dropped by only ca. 30%. Using a compact-tension specimen, 20.0 mm thick, at − 150 °C only alloy F2 satisfied the requirement of plane-strain fracture toughness with a K_{IC} value of 106 MPa $m^{1/2}$. The existence of Cr (4.0%) and the formation of a ferrite phase in an austenite matrix was responsible for the low toughness value observed.

1. Introduction

The development of Fe–Al–Mn alloys is hoped to replace the high-cost alloying elements of chromium and nickel in stainless steels by aluminum and manganese [1,2]. Recent studies indicated that Fe–Al–Mn alloys possesses excellent low [3,4] and high temperature [5,6] properties. It was found [7] that carbon stablized the austenite phase in Fe–Al–Mn alloy and has a profound hardening effect. Thus, the strength of the alloy increases with increasing carbon content. However, there is no data reported on fracture mechanics parameters of the alloys based on linear-elastic fracture mechanics (LEFM) or elastic–plastic fracture mechanics (EPFM). The critical stress intensity factor, K_{IC}, resulting from the LEFM approach is to characterize fracture under plane-strain conditions with attendant small-scale plasticity, while K_C values based on EPFM are to characterize fracture under plane-stress conditions with attendant large-scale plasticity. The K_C value is generally 2–5 times larger than K_{IC} and varies not only with respect to temperature and strain rate, as does K_{IC}, but also with plate thickness [8,9]. The purpose of this research was to study the effect of carbon and chromium contents on the Fe–Al–Mn alloys under plane-strain and plane-stress fracture mechanics conditions at sub-zero temperatures, and to correlate the compositional/microstructural constituents to that of the properties attained.

2. Experimental procedure

Three types of Fe–Al–Mn alloys were tested in this study, of different carbon contents, 0.5, 0.7 and 1.0%. The alloys were homogenized at 1150 °C for 12 h and then hot-rolled to thicknesses of 22 and 10 mm from a 70 mm plate. The plates were subsequently solution heat-treated at 1050 °C for 1 h and then rapidly quenched in water. Aging processes were performed at 500 °C for 4 h. Compact-tension (CT) specimens conforming to ASTM E399 [10] for plane-strain fracture toughness with specimen thickness $B = 20$ mm, and to ASTM E561 [11] for plane-stress fracture toughness with specimen thickness $B = 8.9$ mm, were made by EDM machining. Configuration of the CT specimens were as shown in Fig. 1. A 25 tons capacity MTS hydro-servo dynamic testing machine was used for fatigue pre-cracking and tensile fracturing of the CT specimens. Plane-strain/plane-stress fracture toughness testing were carried out at temperatures of 25, − 50, − 100 and − 150 °C. In addition, tensile tests were also performed with specimen dimension as shown in Fig. 2. Chemical composition of the alloys were analysed by atomic emission spectroscopy, and are listed in Table I. Optical microscopy, as well as X-ray diffraction analysis (XRD), were carried out to identify the phases presented in the materials. SEM fractography was performed on the fracture surfaces of the CT specimens to reveal the fracture morphology of the alloys at various temperatures.

3. Results and discussion

Table I and Fig. 3 show the microstructures of the alloys in this study. It can be clearly seen that F3 alloy possessed the most fine-grained structure among the three alloys. This fine-grained structure may have contributed to the higher elongation and slightly better toughness values obtained, even though its hardness was higher than F1 and F2 alloys. Metallographically, F2 alloy was of ferritic–austenitic duplex structure, where ferrite zones were in blocky form, as marked by arrows in Fig. 3b. F1 and F3 alloys were austenitic single matrices, as confirmed by XRD, Fig. 4a–c. The occurrence of the ferritic phase in alloy F2 is due to the existence of Cr (a ferrite former) in the alloy. The hardness of ferritic zones in F2 alloy is higher than any austenitic phase of the F1/F2/F3 alloys. The solid solution hardening of the Cr in ferrite may have contributed to this effect.

Table II lists the tensile data of the three alloys at various testing temperatures. Despite the microstructural constituents of austenite/ferrite, the tensile strength of the materials seems to be in direct proportion to carbon content, with more carbon giving a higher strength. However, the elongation of F2 alloy was only ca. 50% of the F1 and F3 alloys, due possibly to the presence of the embrittling ferrite phase [13, 14] in the matrix. Like common stainless steel [15], the strength of the Fe–Al–Mn alloys increased while ductility decreased with the decrease of temperature. This can be discerned from Table II and Fig. 5.

Fracture toughness test results of the alloys are tabulated in Table II. CT specimens of 20 mm in thickness were found to be too thin to obtain valid

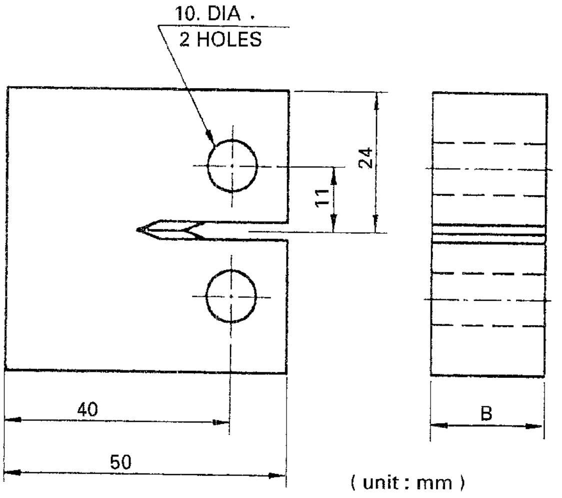

Figure 1 Dimension of the compact-tension specimen for fracture toughness testing. $B = 20$ mm for plane-strain K_{IC} test; $B = 8.9$ mm for plane-stress K_C test.

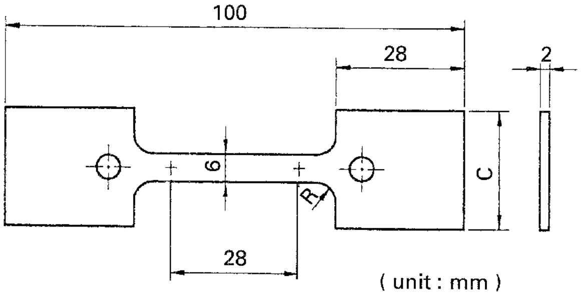

Figure 2 Dimension of tensile specimen for ambient and sub-zero temperature testing.

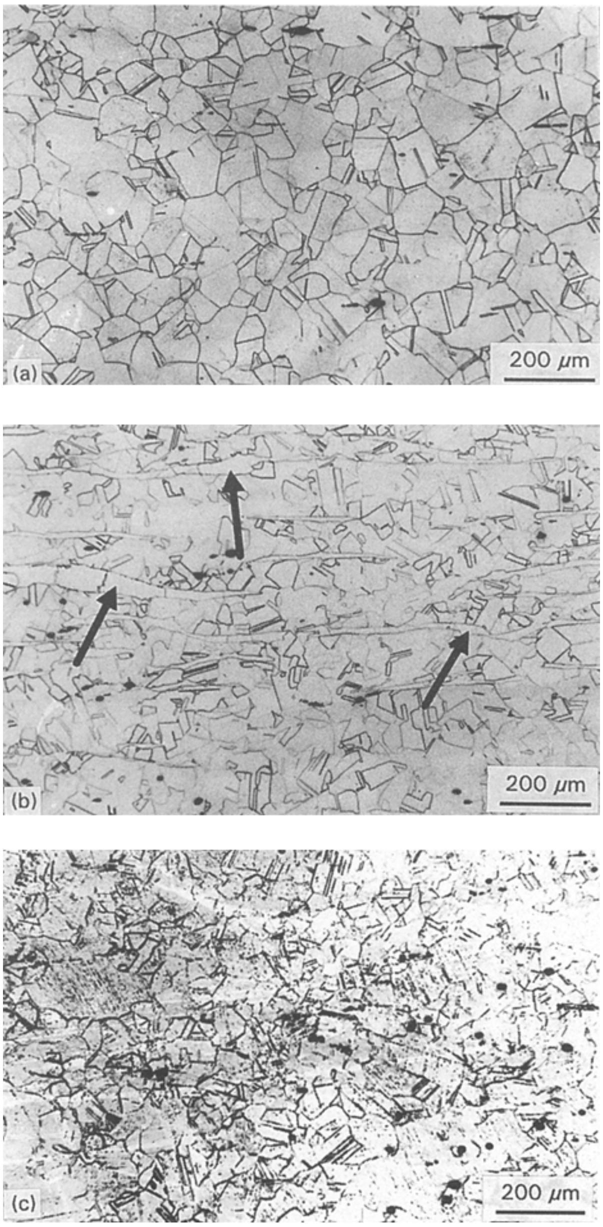

Figure 3 Microstructure of Fe–7Al–27Mn alloys. (a) Austenitic F1 alloy (0.5% C); (b) ferritic–austenitic F2 alloy (0.7% C and 4.0% Cr), the arrows indicate ferritic zones; (c) austenitic F3 alloy (1.0% C).

TABLE I. Chemical composition of the alloys (wt %)

Code	Carbon	Aluminium	Manganese	Chromium	Matrix
Nominal	–	7.0	27.0	–	Austenitic
F1 alloy	0.5	7.5	26.8	–	Austenitic
F2 alloy	0.7	7.8	26.7	4.0	Austenitic + ferritic
F3 alloy	1.0	7.3	26.3	–	Austenitic

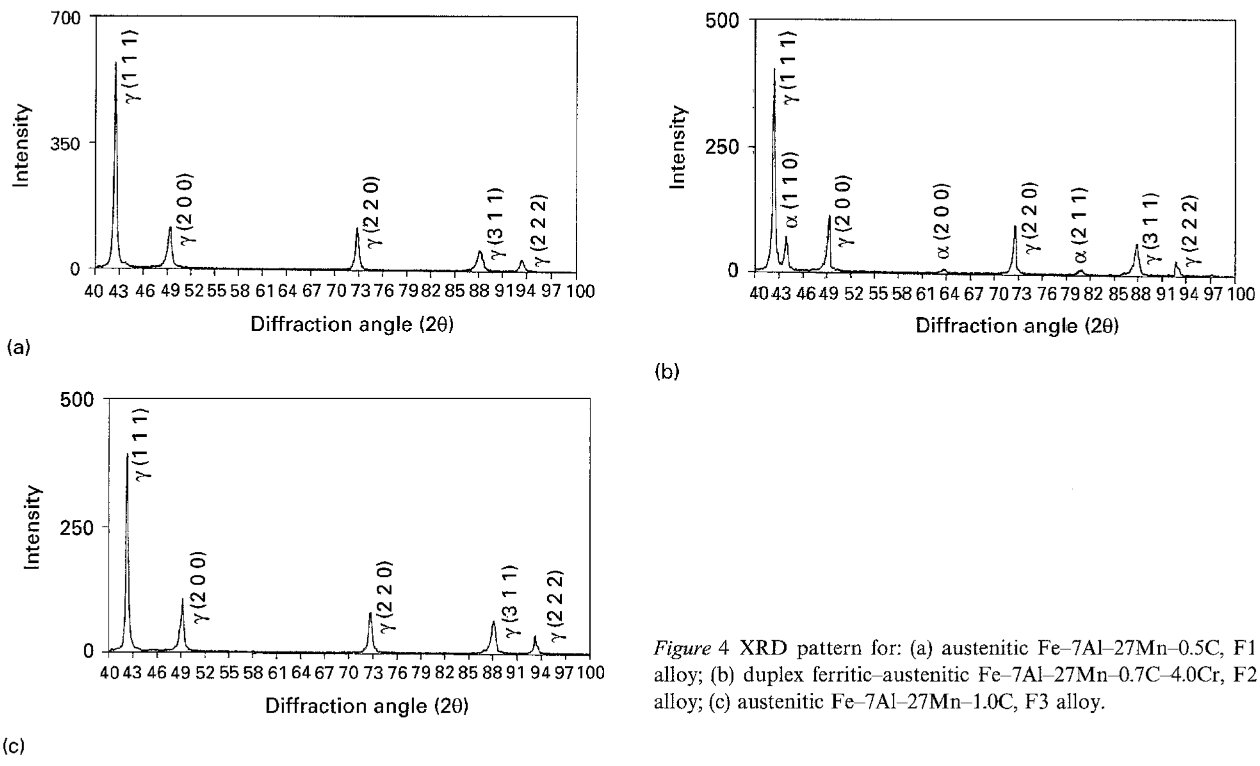

Figure 4 XRD pattern for: (a) austenitic Fe–7Al–27Mn–0.5C, F1 alloy; (b) duplex ferritic–austenitic Fe–7Al–27Mn–0.7C–4.0Cr, F2 alloy; (c) austenitic Fe–7Al–27Mn–1.0C, F3 alloy.

TABLE II Tensile properties and fracture toughness of the alloys

Code	Test temp.	Tensile strength	Elongation	Micro hardness	Plane-strain		Plane-stress	
					K_Q	P_{max}/P_Q	K_c	a_C
unit	(°C)	(MPa)	(%)	H_v(50 g)	(MPam$^{1/2}$)		(MPam$^{1/2}$)	(mm)
F1 alloy	25	896	57	207	52	2.14	448	30.8
	− 50	920	47		65	2.07	414	29.5
	− 100	937	46		74	1.99	377	28.0
	− 150	996	44		126	1.26	275	24.7
F2 alloy	25	968	25	231	68	1.80	331	28.3
	− 50	987	21	261[a]	84	1.58	225	25.0
	− 100	1080	20		97	1.54	197	25.5
	− 150	1220	17		106[b]	1.08	133	19.5
F3 alloy	25	1050	45	253	73	1.83	338	28.2
	− 50	1165	38		90	1.81	285	25.2
	− 100	1173	41		96	1.66	268	24.3
	− 150	1250	35		120	1.35	232	22.4
AISI 4140 [16]					62			
17-7PH Stainless [17]					52			

[a] Micro hardness of ferritic zones (bcc phase).

[b] Valid plane-strain fracture toughness value, $K_Q = K_{IC}$.

K_{IC} values, except for the F2 alloy at − 150 °C with K_{IC} data still very high at 106 MPa m$^{1/2}$. Thus, the austenitic Fe–Al–Mn alloys in this study were of high toughness grades when compared to some of the structural or stainless steels [16, 17]. The toughness comparisons are shown in Table II.

Plane-stress fracture toughness K_C values were then deduced; see Table II and Fig. 5. It was found that F1 alloy (0.5% C) exhibited substantially higher K_C values at all testing temperatures. F1 and F3 alloys, because of the austenitic phase with attendant large-scale crack tip plasticity [1, 14], exhibited superior static toughness properties than F2 alloy. F2 was of duplex phase (austenite and ferrite) structure, where the presence of ferrite (see Fig. 3b) resulted in significant embrittling effects on both toughness and ductility properties.

Figs 6–8 represent the fracture surface morphology of alloys F1–F3, respectively, as observed by SEM. They all exhibited a substantial amount of tearing and dimples at all testing temperatures, signifing that the fracture was of ductile mode, except Fig. 7b of the F2 alloy which showed brittle cleavage facets. Apparently, the ferrite phase within the F2 alloy played a very detrimental role in the low-temperature toughness and ductility property of the Fe–Al–Mn alloys.

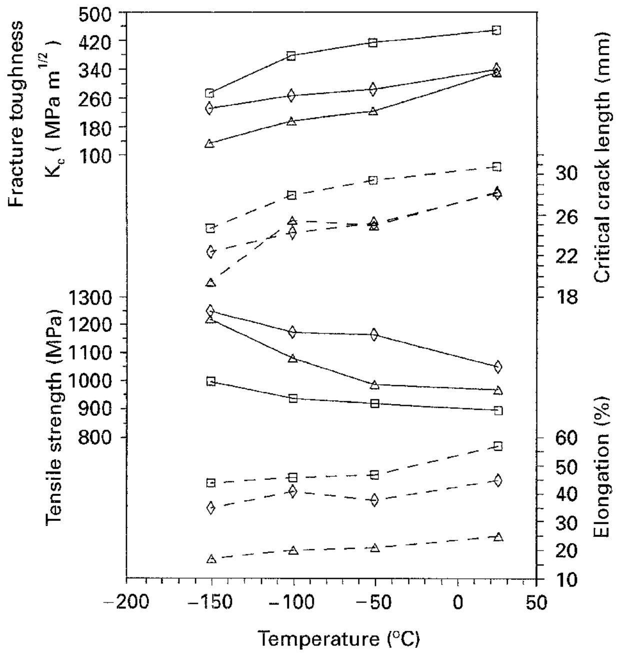

Figure 5 Effects of carbon content and testing temperatures on K_c values and mechanical properties of the Fe–Al–Mn alloys. □, F1 alloy (0.5% C); △, F2 alloy (0.7% C, 4.0% Cr); ◇, F3 alloy (1.0% C).

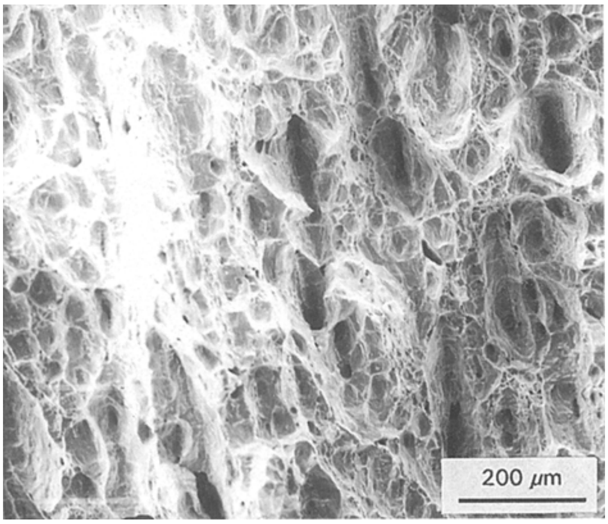

Figure 6 SEM fractomicrographs of the F1 alloy, tensile fracture zone of CT specimen tested at 25 °C.

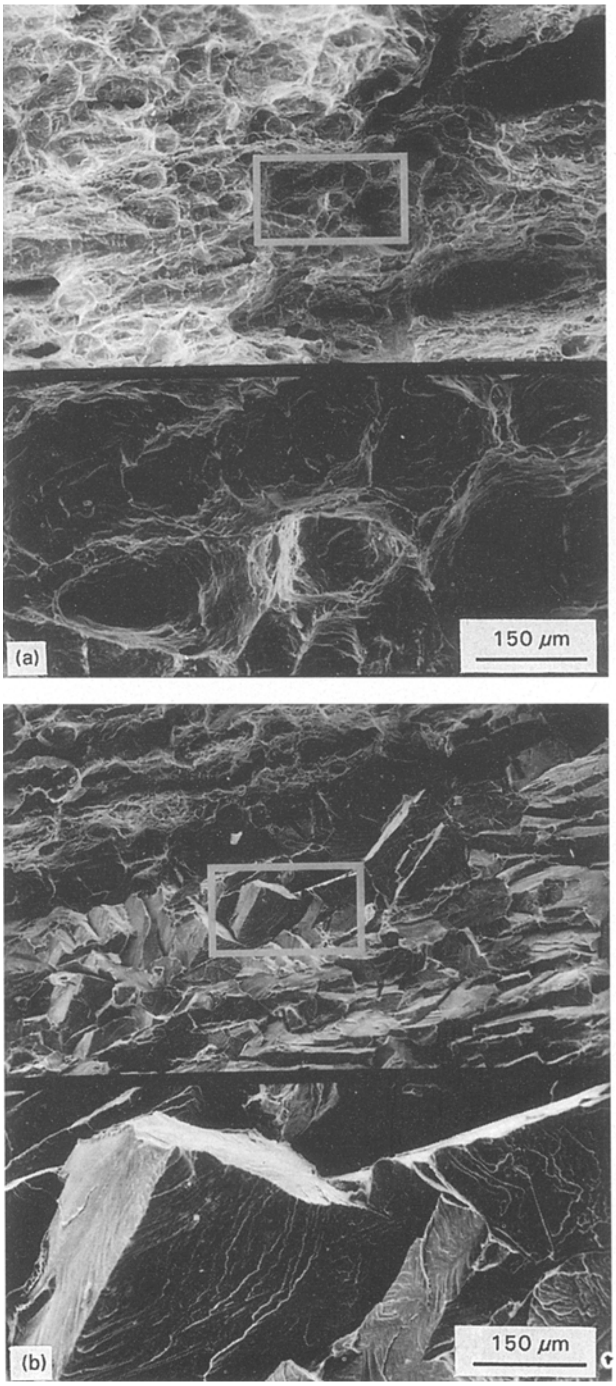

Figure 7 SEM fractomicrographs of the F2 alloy, tensile fracture zone of CT specimens tested at: (a) 25 °C; (b) − 50 °C.

Fe–Al–Mn alloys usually contain particles of precipitated compounds, which contribute greatly to their strength [18, 19]. Figs 6 and 8 reveal typical fractographs of the single phase Fe–Al–Mn alloys. The interface around particles, which are weakly bonded, could easily initiate voids. When the austenitic Fe–Al–Mn alloys were deformed plastically, micro-voids formed around particles and eventually coalesced, which led to the dimpled fracture with corresponding ductile tearing.

The values of the critical crack length, a_c, listed in Table II, represent damage tolerance of the materials to sustain faults before unstable crack propagation starts in the mixed ductile and brittle modes, were also obtained by a compliance procedure based on the relationship [11] :

$$a_C/W = 1.001 - 4.6695(U) + 18.46U)^2 - 236.82(U)^3 + 1214.9(U)^4 - 2143.6(U)^5$$

$$U = 1/[(EBv/P)^{1/2} + 1]$$

where a_c is the critical crack length, W the specimen width, E the modulus of elasticity, B the thickness, v the displacement and P the load.

Apparently, the critical crack length was smaller at lower temperatures when the Fe–Al–Mn alloys became less ductile and not as tough. It is worthwhile mentioning that a_c of the F2 alloy at − 150 °C was 19.5 mm. This value is very close to the fatigue precrack length, a_0, measured as $a_0 = 19.95$ mm after the

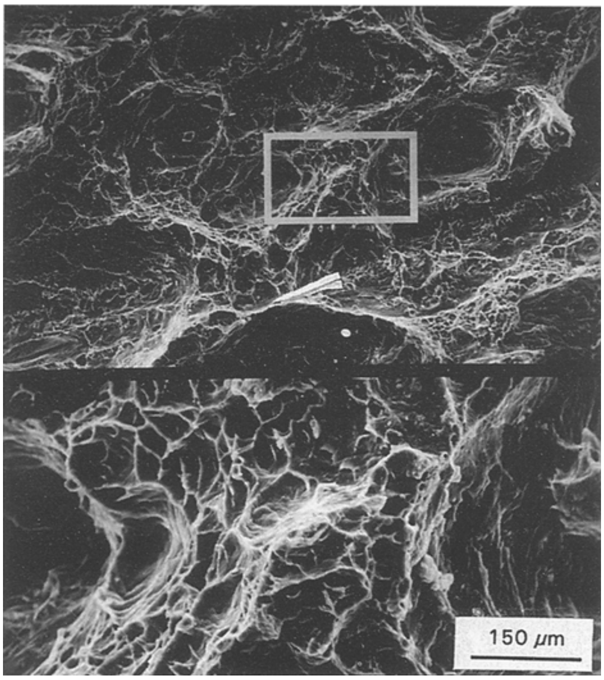

Figure 8 SEM fractomicrographs of the F3 alloy, tensile fracture zone of CT specimen tested at 25 °C.

CT specimen had been pulled apart in fracture toughness testing. Since a_0 was in the vicinity of a_c, unstable and rapid crack propagation resulted in plane-strain failure which met the ASTM requirement for K_{IC} linear-elastic fracture toughness criteria. The linear-elastic behaviour also was most likely to occur when the alloy was of the high strength low ductility at the lowest temperature. This was observed in the present work.

4. Conclusions

Conclusions of this research on low temperature behaviours of the three Fe–Al–Mn alloys investigated can be summarized as follows:

1. All alloys possessed excellent static fracture toughness properties so that only the Fe–7.8Al–26.7Mn–0.7C–4.0Cr (F2) alloy, at − 150 °C, rendered a valid but high K_{IC} of 106 MPa $m^{1/2}$, using compact-tension specimens of 20.0 mm in thickness.
2. The main factor that affects tensile strength and hardness of the austenitic Fe–Al–Mn alloys was found to be carbon content. F3 alloy (1.0% C) possessed the highest strength at the testing temperatures. At sub-zero temperatures, the strength of the alloys increased with an attendant decrease of ductility.
3. While F1 and F3 alloys dropped ca. 30% in K_C fracture toughness and ductility values when the temperature decreased from 25 to − 150 °C, F2 alloy exhibited substantially worse behaviour with ca. 60% drop. The existance of the element Cr and the resulting ferrite phase in the austenitic matrix of the F2 alloy was found to be responsible for the embrittlement effect.

References

1. J. CHARLES, A. BERGHEZAN, A. LUTTS and P. L. DANCOISNE, *Metal Progress* **May** (1981) 71.
2. Y. G. KIM, Y. S. PARK and J. K. HAN, *Metall. Trans.* **16A** (1985) 1689.
3. C. J. ALTSTETTER, A. P. BENTLEY, J. W. FOURIE and A. N. KIRKBRIDE, *Mater. Sci. Engng.* **82** (1986) 13.
4. GLENN T. HADDICK, LARRY D. THOMPSON, EARL R. PARKER and VICTOR F. ZACKAY, *Metal Progress* **Nov.** (1978) 37.
5. W. S. YANG and C. M. WAN, *J. Mater. Sci* **24** (1989) 3479.
6. SAMIR K. BANERJI, *Metal Progress* **April** (1978) 59.
7. S. C. CHANG, Y. S. SHIAU and M. T. JAHA, *J. Mater. Sci.* **23** (1988) 528.
8. S. R. NOVAK, "Resistance to plane-stress fracture of A572 structural steel" STP 591 (ASTM, Philadelphia, 1974).
9. C. F. TIFFANY and J. N. MASTERS, "Fracture toughness testing and its application" STP 381 (ASTM, Philadelphia, 1964).
10. 1993 Annual Book of ASTM E 399–90, Vol. 03.01.
11. *idem.* 561–92a, vol. 03.01.
12. T. F. LIU, C. K. WU and C. C. WU in Proceedings of the 1990 Conference on Research and Development of Fe–Al–Mn, Taiwan, ROC, 1990.
13. SHEN-CHIH LEE and YIN-PEN CHANG, *Chinese J. Metal Heat Treatment* **25** (1989) 38.
14. N. J. HO, L. T. WU and S. C. TJONG, *Mater. Sci. Engng.* **102** (1988) 49.
15. C. VISHNEVSKY and E. A. STEIGERWALD, "Fracture toughness testing at cryogenic temperatures" STP 496 (ASTM, Philadelphia, 1970).
16. W. F. BROWN Jr, "Review of developments in plane strain fracture toughness testing" STP 463 (ASTM, Philadelphia, 1970).
17. MICHAEL BAUCCIO, "ASM Materials Reference Book" (ASM, Ohio, 1993).
18. N. J. HO and S. C. TJONG, *Mater. Sci. Engng.* **94** (1987) 195.
19. T. F. LIU, C. C. WU, J. S. CHOU, Y. L. LIN and S. C. CHEN in Proceedings of the 1989 conference on Research and Development of Fe–Al–Mn, Hsinchu, Taiwan, 1989.

Received 29 June 1994
and accepted 5 April 1995